




Cite this: *Green Chem.*, 2025, **27**, 15291

## Industry-friendly urea coating by interlocking waste proteins and nanoparticles *via* a glass transition approach

Kanchan Swami,<sup>a</sup> Mona Nagargade,<sup>†b</sup> Parul Sharma,<sup>†a</sup> Prem Kumar,<sup>a</sup> Bandana Kumari Sahu,<sup>a</sup> Vishal Tyagi,<sup>b</sup> Sarita Kataria,<sup>a</sup> Navjot Singh<sup>a</sup> and Vijayakumar Shanmugam <sup>\*a</sup>

Sustainable agriculture seeks efficient fertilizers; hence, a stable urea coating using feather particles with zinc oxide nanoparticles as a reinforcing agent is developed through a scalable drum rotor method. Feathers have tensile strength as good as stainless steel, but they lack quick and low-cost processing methods. Hence, acid hydrolysis followed by domestic microwave-assisted thermal treatment is developed, to our knowledge, for the first time, to disperse the feathers into a free-flowing microfiber powder in 10 days. XPS analysis confirmed the formation of keratin–zinc complexes through ionic bonding with carboxyl groups, highlighting the reinforcing role of ZNPs. Optimization of the hydrolysis tuned the glass transition of the feather microfibers to 70 °C, which caused densification and membrane formation during the mild heat-facilitated drum rotor coating. The optimized feather microfiber to ZNPs ratio and subsequent rearrangement significantly enhanced the coating's hydrophobicity and raised the water contact angle to 126°. This densified structure also optimized the Young's modulus, fulfilling critical industrial requirements for stability and controlled release. Importantly, it drastically reduced nitrogen loss in soil, showing <15% leaching loss compared with uncoated urea. The feather microfiber, being recalcitrant and suited for sustained nutrient release in soil, increased the rice yield by ~15%. The chlorophyll analysis using the SPAD value corroborates the yield.

Received 21st August 2025,  
Accepted 15th October 2025

DOI: 10.1039/d5gc04420k

rsc.li/greenchem

### Green foundation

1. A urea fertilizer coating is developed using waste feather protein by leveraging the glass transition temperature, without binders/toxic solvents. Using about 75% of the recommended dose achieves crop production equivalent to 100% uncoated urea; thus, the carbon footprint from intensive Haber urea production can be reduced proportionally.
2. The coated urea shows a reduction in leaching and volatilization and reduced groundwater pollution and greenhouse gas emission, respectively; finally, the biodegradability of the coating is confirmed *via* the soil burial test.
3. The feather microfiber synthesis developed here can be further improved by enzymatic action; the coated fertilizer has to be tested with other combinations and crops.

## Introduction

The global population is predicted to hit 10.1 billion in 2100; therefore, fertilizers will be in high demand.<sup>1</sup> Hence, the UN 17 goals for sustainability insist on fertilizer efficiency through goal 2: zero Hunger, goal 12: responsible consumption and production, and goal 13: climate action. By 2050, urea demand is expected to reach 200 million tonnes. Urea manufacturing

involves N-fixation by the Haber process, which has a huge carbon footprint.<sup>2,3</sup> Volatilization, erosion, surface runoff, and leaching loss are significant for nitrogen fertilizers, which leads to the loss of about 50%–70% of the urea applied to the soil, as there is a mismatch in the rate of crop uptake and nutrient release.<sup>4,5</sup> Additionally, these losses in N-rich fertilizers, such as urea (46% N), result in environmental damage by greenhouse gas emissions (N<sub>2</sub>O and NH<sub>3</sub>) and water eutrophication;<sup>6,7</sup> hence, there is a need to improve the fertilizer use efficiency.

Fertilizer coatings based on synthetic polymers, including polystyrene,<sup>8</sup> polyolefin,<sup>9</sup> polysulfone,<sup>10</sup> and others, were considered for the sustained release of nutrients. To substitute the synthetic polymer, biomass-derived polyurethane made

<sup>a</sup>Institute of Nano Science and Technology, Mohali, Punjab 140306, India.

E-mail: vijayakumarshanmugam@gmail.com

<sup>b</sup>Indian Agriculture Research Institute, Delhi, India

<sup>†</sup>These authors contributed equally to this work.

through a cyanide cross-linker was adopted for urea coatings,<sup>11,12</sup> which guarantee long-lasting release.<sup>13</sup> To make it more robust, the synthesis of polyurethane derived from cotton waste combined with siloxane<sup>14</sup> has been attempted, but in the pursuit of stability, the residual effects were ignored.

The Circular Economy Action Plan under the European Commission proposal limits the polymer use in fertilizer coatings as they need long degradation time, leave microplastic residues, and alter the soil pH.<sup>3</sup>

So biodegradable alternative coatings using lignin + bentonite clay + alginate + polyacrylic acid,<sup>15</sup> silica-coated ligno-cellulose + egg white coating,<sup>16</sup> and other ligno composites have been developed to give stable coatings.<sup>17</sup> In this line of waste-derived fertilizer coatings, modified starch with eggshell nanoparticle coatings has been developed, which are found to be stable.<sup>18</sup> In continuation of this, a couple of chitosan-based systems for phosphorus fertilizer have been developed, in which the latter design demonstrates elegant 4-D slow-release coating characteristics.<sup>19,20</sup> Through sustainable nutrient release during the crop-growing season, this innovation has the potential to boost agricultural output and improve fertilizer use efficiency.

Keratin is the most recalcitrant bio-waste, having tensile strength close to that of stainless steel ( $\sim 250 \text{ MPa Mg}^{-1} \text{ m}^{-3}$ ). It is available in abundance from poultry, given that 65 million tons of chicken are consumed annually worldwide, producing 3–4 million tons of waste feathers.<sup>21,22</sup> Chemically, feathers contain  $\sim 90$ – $92\%$  pure keratin,<sup>23</sup> with an average molecular weight of  $\sim 10 \text{ kDa}$ ,<sup>24</sup> and a linear polymeric backbone having  $\sim 7\%$  cysteine crosslinking sites. Physically, keratin has high tensile strength and good membrane-forming properties.<sup>25,26</sup> The advantage of disulfide cross-linkages to maximize the spinnability of fibers makes feathers suitable for keratin fiber production.<sup>27–30</sup> However, the dispersion of feathers as fine particles suitable for film formation requires toxic linker, surfactants such as SDS,<sup>29</sup> reductants such as L-cysteine,<sup>26</sup> or alkali solvents, which restrict the commercial potential.<sup>31</sup> Barone, in 2006, developed a scalable method by tuning the extrusion temperature to form a viscous dispersion suitable for film formation, which gained industrial appreciation.<sup>32</sup>

Here, another scalable alternative was studied in which feathers were dispersed quickly into a coating-compatible powder by acid hydrolysis coupled with microwave thermal treatment and drying. Further, the glass transition ( $T_g$ ) temperature of keratin was explored for fertilizer coating, generally  $T_g$  lie in the range of 67 to 100 °C based on the degree of hydrolysis and the classical rule to engage binder to form a stable coating has been waived.<sup>33</sup> A high concentration of keratin in glassy state is known to promote efficient binding.<sup>34</sup> This will enable the industry to comply with the environmental regulations and prevent nutrient loss during processing.

The critical role of nanostructures in the future circular economy<sup>35</sup> encourage to capitalise the ability of nanoparticles to reinforce membranes for stability. Therefore, in this study,

to achieve a feather microfiber biopolymer coating on a fertilizer, nanoparticles were used as the reinforcement agent. Zinc is an essential micronutrient, and zinc oxide nanoparticles have been utilized in deficient soil, particularly in rice and corn production.<sup>36,37</sup> Thus, ZnO nanoparticles have been employed as the reinforcement agent here. The ability of cationic Zn to coordinate in a multidentate fashion with thiols, amines, and hydrocarbons in the keratin is expected to aid successful reinforcement.<sup>38–40</sup> While, on the application side, zinc plays two important roles: first, it acts as a cofactor in many physiological functions,<sup>41–43</sup> and, second, it is involved in defence responses and signalling in plants, which is regulated through zinc finger proteins and ROS metabolism.<sup>44,45</sup> Hence, its addition in the coating is expected to complement crop productivity. Furthermore, for the first time, the glass transition temperature of keratin is used for the coating, which enables a binder-free coating (Table 1) on urea pellets *via* a drum rotor method. The product has been tested for crop production efficiency in rice.

## Experimental

### Materials

Urea (46% nitrogen) was bought from IIFCO to carry out the coating with poultry feather microfibers (treated with 0.001% sulfuric acid for 10 days, followed by microwave treatment). Materials such as petroleum ether, isopropyl alcohol, and soda ash ( $\text{Na}_2\text{CO}_3$ ) were purchased from RANKEM; Soda ash lime sequestering agent (CaOH) and zinc acetate from SRL; Potassium hydroxide from HIMEDIA; and ethanol from Thermofisher chemicals. All the chemicals were of analytical grade.

### Preparation of coating material

**Extraction of feather microfiber (KPP).** Given that poultry feathers are composed of  $\sim 90$ – $92\%$  keratin protein, they must be used as a whole without any extraction, which would merely result in loss.<sup>23</sup> Owing to the complexity of the feather's structure, it became apparent that grinding them for further use was challenging. Previously, protein extracted from feather waste involved several lengthy and intricate procedures, and the yield was often insignificant.<sup>26,48</sup> Hence, here, raw feathers

**Table 1** Coating materials and their binder/cross-linkers

Coating materials	Binder/cross-linker	Ref.
Bio-based polyurethane acrylate (BPUA), polydimethylsiloxane (PDMS), and thiol-grafted nanosilica (TNS)	BPUA <i>via</i> UV curing	46
Bio-based polyurethane (from liquefied wheat straw), organosilicon, and nano-silica	BPU thermally crosslinked polymer	47
Chitosan and citric acid	Citric acid	20
Waste feather and ZnO nanoparticles	Binder-free	Present study

were first pretreated with the standard ASTM D 584 procedure,<sup>49</sup> then briefly rinsed with deionized water and dried at 40 °C, followed by Soxhlet treatment<sup>50</sup> using petroleum ether at 70 °C to remove oil. Further, the pre-processed dried feathers were immersed in 0.001% sulfuric acid solution (100 mL g<sup>-1</sup>) at pH 5 maintained for 10 days to achieve mild hydrolysis and dispersion without significantly damaging the protein structure. The resultant material was microwave-treated for 45 minutes, halting every 5 minutes, using a standard domestic microwave oven operating at ~700 Watts (standard power for domestic microwaves). After this treatment, the material loses its firmness and is subsequently ground to a fine powder using a ball mill for 6 hours at 320 rpm, with an interval of 15 minutes after each hour.

**Synthesis of zinc oxide nanoparticles (ZNPs).** Zinc oxide nanoparticles (ZNPs) were synthesized by a co-precipitation method with minor modification.<sup>51</sup> Briefly, 0.779 g of zinc acetate (precursor) was mixed with 42 mL of anhydrous ethanol and 0.25 mL of water. This solution was incubated at 80 °C under inert conditions. Separately, a potassium hydroxide solution was prepared by dissolving 0.442 g of KOH in 23 mL of ethanol and added drop-wise to the zinc acetate mixture. After 16 h of reaction, the flask was allowed to cool to ambient temperature, and the synthesized ZNPs were dispersed and washed in a 1 : 1 solution of isopropyl alcohol and ethanol. Finally, the particles were pelleted down by centrifugation. Upon drying at 60 °C, the resultant ZNPs were again dispersed in a 10% ethanol solution for coating.

#### Preparation of coated urea pellets

The urea pellets (average diameter 3–4 mm) were screened using 4 mm and 3 mm pore size sieves. The resultant pellets were weighed and placed in a customized rotatory drum operated at 70 °C and 32 rpm. While the rotation was in progress, a high-pressure air gun was used to spray ZNPs in 10% ethanol (so that it is in the powder state when it reached the pellet) followed by feather microfiber onto the urea pellets. The rotor was rotated at 32 rpm for an additional 30 minutes after the heater was switched off. After the coating was completed, the coated urea pellets were collected. Three different thicknesses of coated urea pellets, designated as KZC1, KZC2, and KZC3, corresponding to 3%, 6%, and 10% of the coating materials, respectively, were prepared. The coating percentage was determined using eqn (1).

$$\text{Coating percentage} = \{w_2 - w_1/w_2\} \times 100 \quad (1)$$

where  $w_1$  is the weight of the uncoated urea pellets and  $w_2$  is the weight of the coated urea pellets.

#### Characterization of the coating material

A Bruker D8 Advance powder XRD (X-ray diffractometer) with Cu-K $\alpha$  radiation ( $\lambda = 1.5406 \text{ \AA}$ ) at 40 kV and 25 mA was used to record the diffraction peaks of ZnO particles and examine the crystalline behaviour of the coating material. A Bruker Vertex 70 series Fourier transform infrared (FTIR) spectrometer in

attenuated total transmittance mode was used to perform spectrum analysis. A TA Instruments Differential Scanning Calorimetry (DSC) Q2000 V24.11 was used to determine the glass transition temperature of the synthesized feather microfiber. Scanning electron microscopy (SEM) images were captured using a JEOL JSM IT300 device operating at 15 kV. UV-visible absorbance spectra were recorded using an Agilent Technologies Spectrophotometer. The zeta potential of the material was recorded using a Malvern Zetasizer instrument. A JASCO J-1500 spectrometer was used to record the circular dichroism (CD) spectra using a quartz cuvette with a 2 mm path length, 190–400 nm wavelength range, and 200 nm min<sup>-1</sup> scan rate. The N<sub>2</sub> adsorption–desorption analysis was performed with a Quantachrome Autosorb iQ2 Brunauer–Emmett–Teller (BET) surface analyzer at –196.15 °C. A confocal Raman system (WITEC focus innovation) was used to record the Raman spectra at 532 nm laser wavelength and 10 mW power. A Thermo Scientific K-Alpha surface analyzer coupled with a monochromatic Al-K $\alpha$  source ( $h = 1486.6 \text{ eV}$ ), a micro-focused (400  $\mu\text{m}$ , 12 000 V, 72 W) hemispherical analyzer, was used to perform X-ray photoemission spectroscopy (XPS) studies. The mechanical property of the coated composite in terms of Young's modulus were determined using an Anton Parr MCR302 Rheometer configured with a 50 mm parallel plate geometry to obtain stress–strain curves. A Kruss Advance drop-shape analyzer (DSA) was used to measure the hydrophobicity of the coating material by water contact angle measurements. Molecular docking was performed with AutoDock Vina 112, which simulates the molecular interactions in 3D space, and BIOVIA Discovery Studio Visualizer was used for the visualization of the bonds as well as the docked structure.

#### Characterization of coated urea pellets

The mechanical strength was evaluated by investigating the penetration and abrasion strength of the coated urea pellets (KZC1, KZC2, and KZC3) in comparison to uncoated urea pellets.

**Penetration strength.** A commercial table-top penetrometer (Khera) was used to perform the penetration study. The penetration distance in units of 1/10th mm was calculated from the difference between the initial and final values obtained after placing each pellet (10 for each coating) on a flat surface and subjected to pressure with a 70 g plunger connected to the penetrometer.<sup>16,18</sup>

**Abrasion strength.** Abrasion resistance measurements were conducted following the Fertilizer Manual published by the International Fertilizer Development Centre (IFDC S-116) of the United Nations Industrial Development Organization.<sup>52</sup> Briefly, a cylindrical container containing zirconium beads and 10 g of weighed pellets (3 : 1) was placed within a rotating drum at 30 rpm. The pellets were taken out after 2.5, 5, 10, 20, and 40 minutes and sieved through 3 and 1 mm pore-size sieves. The pellets that were left over the 1 mm sieves were then collected at regular intervals and weighed. The abrasion%

was determined by using eqn (2), and the experiment was run in triplicate.

$$\text{Abration\%} = 100 - 100(m_2/m_1) \quad (2)$$

where  $m_1$  is the weight of pellets added to the cylinder and  $m_2$  is the weight of the pellet recovered after abrasion.

**Humidity strength.** The pellets (10 for each coating) were incubated at different relative humidity levels (40%, 50%, 60%, 70%, and 80%) in a humidity-controlled incubator (Scientific Instrument) for 20 days and weighed before and after incubation time, then analyzed gravimetrically.<sup>53</sup> The water permeability of the coated (KZC1, KZC2, and KZC3) and uncoated urea pellets was calculated by using eqn (3) and was monitored regularly.

$$\text{Water permeability\%} = 100 - (m_1/m_0) \times 100 \quad (3)$$

where the weights of the urea pellets at 20 and 0 days were denoted by  $m_1$  and  $m_0$ , respectively.

**Water-holding strength.** The capacity of the coating to hold water in the coated pellets (KZC1, KZC2, and KZC3) was estimated by swelling%, where gravimetric analysis was performed before and after soaking the pellets in water for 24 hours. The weight change of the pellets was then converted into swelling percent<sup>54</sup> using eqn (4). Each treatment was performed in triplicate:

$$\text{Swelling\%} = [(s_1 - s_0)/s_0] \times 100 \quad (4)$$

where  $s_0$  is the pre-test weight and  $s_1$  is the post-test weight.

**Biodegradability study.** A soil burial test was performed using the soil processed after carefully separating stones, debris, and hardened clumps. The coating was performed in triplicate on a glass slide in the same way as on urea pellets by using an air-gun; following this, the slides were dried, weighed, and placed at a depth of 5 cm in the soil. At regular intervals, the soil was irrigated to maintain field capacity. The coated glass slides were drawn out of the soil at regular intervals, *i.e.*, 10, 20, 30, 40, 50, and 60 days, to record the weight.<sup>16,55</sup> The weight loss percentage was used to determine the biodegradability of the coating composite. The weight loss was calculated using eqn (5).

$$\text{Weight loss\%} = [(m_1 - m_2)/m_1] \times 100 \quad (5)$$

where  $m_1$  is the slide's pre-test weight and  $m_2$  is the film's post-test weight.

**Cumulative release study.** The nitrogen release experiment was performed in triplicate by incubating 10 g of coated (KZC1, KZC2, and KZC3) and uncoated urea in 200 mL of distilled water at room temperature.<sup>6,56</sup> At regular intervals, 2 mL of the sample was withdrawn and concurrently refilled with the same amount of water. Nitrogen was estimated from the collected samples, with the help of Kjeldahl apparatus (Tulin KjelTron).

**Mechanism study.** The kinetics of nitrogen release was determined using four mathematical models represented in the following equations, where,  $A_t$  denotes the cumulative

release rate at time  $t$ ,  $A_0$  is the maximum release rate,  $b$  is the release constant,  $t$  is the release time,  $M_t/M_0$  is the urea release rate at time  $t$ ,  $k$  is the diffusion constant, and  $n$  is the diffusional exponent, which describes the transport mechanism (Table 2).

The coefficient of determination ( $R^2$ ) and the standard error of estimates (SER) were calculated to finalize the best-fitting model.<sup>51</sup> The standard error of estimation (SER) is determined using eqn (6), where  $n$  represents the number of experimental data,  $Nt$  is the experimental value, and  $Nt'$  is the calculated value.

$$\text{SER} = \left\{ \sum [(Nt - Nt')^2 / (n - 2)] \right\}^{0.5} \quad (6)$$

Here  $n$  depicts the flow kinetics; if  $n \leq 0.5$ , Fickian diffusion-controlled release occurs, and if  $n$  is between 0.5 and 1, it indicates a non-Fickian diffusion release mechanism.

**Leaching loss study.** To compute the leaching loss of nutrients from the fertilizer pellet, a well-drenched loamy soil column with a pH of 7.2 was packed in a PVC column. In this column, the coated (KZC1, KZC2, and KZC3) and uncoated pellets were incubated in triplicate for 40 days. During this incubation time, the leachates were collected at periodic intervals (0, 5, 10, 20, 30, and 40 days) while keeping soil moisture in a saturated condition by irrigating every 2 days.<sup>56,57</sup> The percentage of nitrogen in the leachates was estimated using the Kjeldahl method.

**Volatilization loss study.** Volatilization loss of nitrogen as ammonia was calculated using a Keithley DMM6500 6 1/2 digit multimeter through the chemoresistive method. The percentage of volatile ammonia loss from the coated (KZC1, KZC2, and KZC3) and uncoated urea pellets was determined using the resistance signal from a typical  $\text{SnO}_2$  ammonia sensor, represented as sensor response (SR) at 150 °C and 50% relative humidity.<sup>18,58</sup>

$$\text{SR} = (R_{\text{air}}/R_{\text{gas}}) - 1 \quad (7)$$

Here  $R_{\text{air}}$  is the resistance in synthetic air, and  $R_{\text{gas}}$  represents the resistance in the presence of coated and uncoated urea pellets.

### Pot study

**Treatment details.** After the lab study, the effectiveness of coated urea pellets over uncoated pellets was evaluated in a pot experiment on rice crops (var. PB1509). A total of 15 pots (3 replications of each treatment) were arranged and filled with 25 kg of farm soil in each pot. Before filling the soil into

**Table 2** Mathematical models and equations to determine the mechanism

Model	Equations
First-order	$A_t = A_0(1 - e^{-kt})$ or $\ln(A_0 - A_t) = \ln(A_0) - kt$
Simple-Elovich	$A_t = b + k \ln t$
Parabolic diffusion	$A_t = b + kt^{0.5}$
Ritger-Peppas	$M_t/M_0 = kt^n$ or $\ln(M_t/M_0) = \ln k + n \ln t$

**Table 3** Treatment details of the pot study

Treatment	Dose w.r.t. the recommended dose	Time of application
Control	100% recommended dose of N (RDN)	1/3 <sup>rd</sup> basal + 1/3 <sup>rd</sup> active tillering + 1/3 <sup>rd</sup> panicle initiation
T1-100-B + AT	100% RDN	1/2 basal + 1/2 active tillering
T2-100-B + AT + PI	100% RDN	1/3 <sup>rd</sup> basal + 1/3 <sup>rd</sup> active tillering + 1/3 <sup>rd</sup> panicle initiation
T3-75-B + AT	75% RDN	1/2 basal + 1/2 active tillering
T4-75-B + AT + PI	75% RDN	1/3 <sup>rd</sup> basal + 1/3 <sup>rd</sup> active tillering + 1/3 <sup>rd</sup> panicle initiation

the pots, the soil was analyzed for its nutrient content. From the rice nursery bed, 25-day-old rice seedlings were transplanted with 4 seedlings per pot. Sufficient moisture was maintained throughout the crop cycle. Coated fertilizers (KZC) were applied as per treatments (Table 3).

### Plant studies

At maturation of the rice (panicle-yellowing stage), the crop was harvested individually for each treatment, packed, and marked carefully. After that, the harvested material was sun-dried to achieve an ideal moisture content for threshing, and grain yield was calculated by gravimetric analysis of grains in grams. The percentage yield increase of each treatment over the control was calculated using eqn (8).<sup>56</sup>

$$\text{Increased yield}\% = \left[ \frac{\text{treatment yield} - \text{control yield}}{\text{control yield}} \right] \times 100 \quad (8)$$

The calculated straw yield accompanied the determination of grain yield in a similar manner. The Harvest index (HI) was determined using eqn (9) after calculating both grain yield (economic yield) and biological yield.

$$\text{HI}\% = \left[ \frac{\text{economic yield}}{\text{biological yield}} \right] \times 100 \quad (9)$$

### SPAD value and nutrient analysis of plant samples

The N content in the vegetative parts (above ground) was estimated using the Kjeldahl method at 30 and 60 days after sowing. The samples were collected, dried, and then used for N% estimation. A SPAD-502, a handheld chlorophyll meter (Minolta Corporation, Ramsey, N.J.), was used for non-destructive and rapid estimation of chlorophyll content in the green leaves. Furthermore, zinc content in grains and straw was determined by the wet-digestion (diacid-digestion) method.<sup>59</sup> Zinc utilization efficiency (ZUE) was computed using the following formula:

$$\text{ZUE} = \text{physiological efficiency (PE)} \times \text{apparent recovery efficiency (ARE)} \quad (10)$$

where PE = (grain and straw yield of treatment – grain and straw yield of control)/(zinc uptake in grain and straw of treatment – zinc uptake in control), and ARE = (zinc uptake in grain and straw of treatment – zinc uptake in control)/(total amount of zinc applied).

### Life cycle assessment (LCA)

Life Cycle Assessment (LCA) was performed using openLCA 2.0.2 software developed by GreenDelta, with data sourced from theecoinvent database.<sup>60</sup> The assessment mainly focused on evaluating the life cycle of raw materials used in the coating of urea and their associated environmental impacts across multiple categories. A cradle-to-gate system boundary was adopted, encompassing all stages, from raw material extraction to the production of the final coated fertilizer. For comparative analysis, conventional industry-standard coatings, sulfur-coated, and polymer-coated urea fertilizers were assessed. The Life Cycle Impact Assessment (LCIA) was carried out to quantify impacts across several key environmental factors, including freshwater ecotoxicity, human carcinogenic toxicity, marine ecotoxicity, ozone formation (both human health and terrestrial ecosystems), terrestrial acidification, and terrestrial ecotoxicity.

### Statistical analysis

The pot culture study was performed using a randomized block design, and all experiments were carried out in replicates. Origin software (OriginPro 2024) was used to plot the graphs, and one-way ANOVA was carried out to evaluate the data's significance.

## Results and discussion

The aim of this study was the sustained release of urea using poultry waste feathers as the coating, reinforced with zinc oxide nanoparticles through an industrially scalable drum rotor coating method. For spraying compatibility, for the first time to our knowledge, the feathers were powdered through scalable microwave heating. Thus, the synthesized feather microfibers (KPPs) and ZNPs were powder-coated onto the urea pellets using a high-pressure air gun for sustained nutrient release.

### Characterization of the coating material

Feathers, composed of keratin, have a secondary structure comprising  $\alpha$ -helix and  $\beta$ -sheets, which is formed by disulfide linkages, which makes it both robust and recalcitrant.<sup>61</sup> For any application of this pure protein waste (90% keratin), the feather is pre-processed using di-2-mercaptoethanol and L-cysteine. About a decade ago, a scalable mechanical feather dispersion process was developed for film formation by tuning the extrusion temperature.<sup>32</sup> This motivated us to develop a

relatively facile process that involved hydrolysis by acid, followed by microwave thermal treatment. This treatment does not damage the protein structure completely, which is evident from the XRD spectra observed before and after the hydrolysis, microwave heating, and milling process (Fig. 1a). As the  $2\theta$  peaks of KPP show only a minor change, such as a drop in the  $9^\circ$   $2\theta$  intensity and shift in the  $20^\circ$   $2\theta$  peak towards higher angle with broadening, which correspond to lower  $\alpha$ -helix and higher  $\beta$ -sheets/ $\beta$ -turns, respectively.<sup>62</sup> Corroborating this, TEM images show a sheet-like morphology (Fig. S1). Following this, FTIR spectroscopy revealed that the chemical structure and groups remained intact before and after the processing (Fig. 1b). As the characteristic absorption bands of amide I (–CONH–) (C=O stretching vibration) at  $1700\text{--}1600\text{ cm}^{-1}$ , amide II (N–H bending and C–H stretching vibration) at  $1531\text{ cm}^{-1}$ , amide III (in-phase C–N stretching and N–H in-plane bending) at  $1220\text{--}1300\text{ cm}^{-1}$ , and asymmetric and symmetric S–O stretching vibrations at  $1167$  and  $1073\text{ cm}^{-1}$  were retained.<sup>63,64</sup> Thus, the hydrolysis was tuned in such a way that the physical and chemical structures are primarily retained, with the  $T_g$  tuned to  $70^\circ\text{C}$  so that it matches the heating in the process of the drum-rotor-assisted fertilizer coating (*vide infra*) (Fig. S2). ZNPs were synthesized using the co-precipitation method, forming zincite (syn) nanoparticles. The XRD analysis confirmed the pattern to be consistent with the JCPDS spectra no. 00-0361-1451, which corresponds to hexagonal lattices (Fig. 1c). The SEM image shows spherical nanoparticles with an average diameter of  $\sim 29\text{ nm}$  (Fig. 1d, 1d inset). The FTIR spectrum shows sharp bands at  $511\text{ cm}^{-1}$  and  $433\text{ cm}^{-1}$  corresponding to the stretching vibration of the Zn–O bond, and the UV spectrum shows absorption maxima at  $365\text{ nm}$ , corresponding to the bandgap of the ZNPs (Fig. S3 and S4).<sup>65,66</sup>

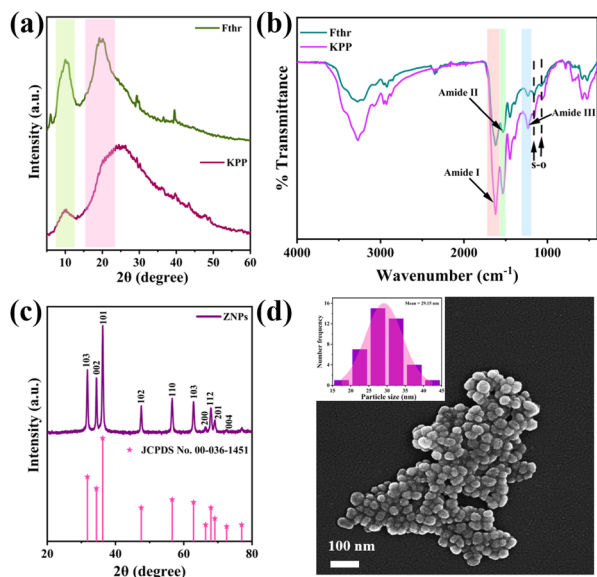


Fig. 1 (a) XRD and (b) FTIR spectra of feather microfiber (KPP) and feather (Fthr), (c) XRD spectra and (d) SEM image with inset of size distribution graph of ZnO nanoparticles (ZNPs).

## Chemical nature of the coating

The synthesized feather microfiber and ZNPs, were powder-coated over urea [(500 ppm ZNPs in  $100\ \mu\text{L}$  +  $300\text{ mg}$  feather microfiber)  $10\text{ g}^{-1}$  urea] (the ratio and the volume has been optimized for even coating *vide infra*). The physicochemical properties of this blend were characterized using XRD, CD, SEM and BET, which confirmed the presence of ZNPs in the polymer framework. The XRD spectra of the coating show broad humps at  $2\theta = 20^\circ$ , signifying higher  $\beta$ -sheets,  $\beta$ -turns, and random coil<sup>62</sup> overlapped with crystalline ZNPs peaks corresponding to 100, 002, and 101 *hkl* planes (Fig. S5). The spectra also confirm the semi-crystallinity, which may greatly influence coating flexibility. The CD spectra show the typical  $\alpha$ -helix and  $\beta$ -sheets of the keratin secondary structure in the feather microfiber sample. The addition of ZNPs led to a significant redshift in the negative  $215\text{ nm}$   $\beta$ -sheets peak and an appearance of a positive  $225\text{ nm}$  random coil peak, which is attributed to the denaturation and re-conformation to a new structure (Fig. 2a).<sup>67,68</sup> Additionally, zinc acts as a nano-filler, as seen in the SEM micrograph image showing filled pores on the protein sheets (Fig. 2b inset); this behaviour reflected a noticeable drop in surface area from  $22\text{ m}^2\text{ g}^{-1}$  to  $4\text{ m}^2\text{ g}^{-1}$  by BET analysis after the ZNPs were introduced (Fig. 2b).

To understand the bond formation in the coating material, the composite was characterized using XPS, ZETA, FTIR and Raman spectroscopy. XPS analysis confirms the elements and the bond formation of zinc with the carboxyl group of the protein in the coating composite. The presence of the main components of KZC, *viz.*, C, O, N, and Zn, was confirmed in the photoelectron survey scan (Fig. 3a). Furthermore, comparison of the KPP and KZC in the narrow-scan spectra of oxygen (Fig. 3b and c, respectively) shows the appearance of a new peak at  $529.78\text{ eV}$  that is indicative of ionic bond formation between zinc and the carboxylic group on the protein. Furthermore, the COOH percentage at  $531.607\text{ eV}$  decreases after linking with zinc, which allows the unreacted percentage



Fig. 2 (a) CD spectra and (b) BET isotherm graph of feather microfiber zinc coating material (KZC) and feather microfiber (KPP). The inset shows the SEM image before and after filling pores in KPP and KZC, respectively.

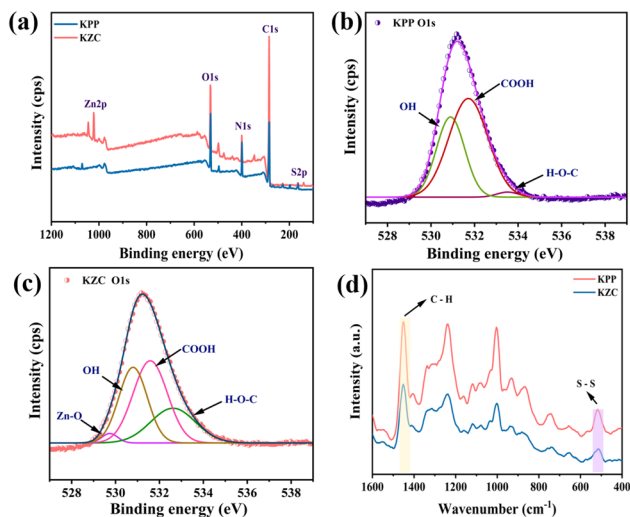


**Fig. 3** (a) XPS and (b) narrow XPS spectra of oxygen (O 1s) of feather microfiber (KPP) and (c) feather microfiber zinc coating material (KZC). (d) Raman spectra of feather microfiber (KPP) and feather microfiber zinc coating material (KZC).

of C–OH to expose and increase,<sup>69,70</sup> confirming that the protein forms a complex with the zinc ion by removing a proton from the carboxylic acid. Finally, the binding energy of O–H decreased from 530.9 eV to 530.68 eV. The relationship between the average oxygen charge ( $Q$ ) and binding energy (BE) was calculated to confirm the binding of zinc with the carboxyl group rather than the hydroxyl group of the protein by the following formula.<sup>68</sup>

$$Q = -4.372 + [385.023 - 8.976 \times (545.509 - \text{BE})]^{1/2} / 4.488 \quad (11)$$

The magnitude of  $Q$  increased as the binding energy decreased. Consequently, the increased electron density around the oxygen atom decreased the proton dissociation from the hydroxyl group, making it hard to break that bond and link with zinc. Therefore, carboxylate ligands were identified as 1° metal acceptors. It was confirmed that complexes are formed by the elimination of a proton (hydrogen) between metals and carboxyl groups. To support the obtained results, molecular docking was performed, which revealed significant interactions between  $\text{Zn}^{2+}$  and specific amino acid residues of the keratin protein, such as glutamine and serine. These interactions support the XPS results. Notably, the docking data showed a metal-acceptor bond formation between  $\text{Zn}^{2+}$  and the carboxyl oxygen (OE2) of the protein (Glu418) (Fig. S6), and the distances of interaction were found to be 2.43–5.54 Å between the docked protein and the zinc ion (Table S1). These findings corroborate the proposed binding mechanism in which  $\text{Zn}^{2+}$  primarily interacts with deprotonated carboxylic acid groups, supporting the hypothesis of keratin– $\text{Zn}^{2+}$  complexation at the molecular level.

The zeta potential measurement of feathers without ZNPs and with the ZNPs shows the shift in the surface charge from a strong negative potential to a weak negative potential (Fig. S7).

This shift may be due to ionic bond formation between the carboxylic groups and  $\text{Zn}^{2+}$  ions in the ZNPs, which reduces the negatively charged carboxyl ends. The FTIR spectra show the coexistence of amide bands as well as bands for ZnO and S–O stretching (Fig. S8). However, there is no change in the amide bands compared to the feather fiber without ZNPs, which negates any coordination with the amide. Comparison of the Raman spectra of KPP and KZC samples shows no change in the 500  $\text{cm}^{-1}$  and 1450  $\text{cm}^{-1}$  peaks corresponding to S–S bonds and C–H bonds, which once again confirms the chance of zinc binding to thiol or C–H bonds to be remote, and is thus limited to the abundant –COO groups.<sup>27</sup>

### Physical nature of coating

Three different thicknesses of the urea pellet coating were obtained using 3%, 6%, and 9% of coating content, denoted as KZC1, KZC2, and KZC3 in the following text, respectively. Coating thickness was determined from the SEM cross-sectional micrograph image. With the increase in coating content, the thickness was found to be  $\sim 43.9 \mu\text{m}$ ,  $\sim 45 \mu\text{m}$ , and  $\sim 45.7 \mu\text{m}$  for KZC1, KZC2, and KZC3, respectively. Protein coating without the nanoparticles, *viz.*, KC alone, shows a thickness of  $\sim 47.8 \mu\text{m}$ , but did not show adhesion, and was therefore found to be unstable due to the absence of a structure-stabilising nano-filler (Fig. 4). The coating is expected to give hydrophobicity and flexibility to enable controlled release as well as stability during transport and storage. The impact of thickness on the flexibility and hydrophobicity of protein coatings without nano-filler (KC) and with nano-filler (KZC1, KZC2, and KZC3) was compared. Flexibility was determined using Young's modulus calculated from the stress–strain curve slope. Young's modulus measurements revealed that the initial incorporation of ZnO nanoparticles (KZC1) further reduced the Young's modulus from KC. This may be due to two reasons: (i) additional structural changes, including a decrease in  $\beta$ -sheet content and the appearance of random coils, which likely resulted from the initial disruption of the keratin structure upon the addition of the nanoparticles. (ii) The initial incorporation of ZNPs at an overall lower concentration might disrupt the inherent self-assembly. However, as



**Fig. 4** Cross-sectional SEM images showing the average thickness of (ai), (aii) feather microfiber coated with urea as a control coating (KC), and (bi), (bii); (ci), (cii); and (di), (dii) three different feather microfiber zinc-coated urea samples with 3%, 6%, and 9% coating content (KZC1, KZC2, and KZC3), respectively.

the coating content (overall zinc concentration) increased in KZC2 and KZC3, the effect of compaction related to the elasticity of the material was found to be more prominent, leading to the appearance of a more compact framework where the nanoparticles act as effective nano-fillers within the polymer framework and overpower the effect of structural alteration. In these higher concentrations, the nano-fillers lead to an increased Young's modulus and thus complement the overall structural integrity of the coating (Fig. 5a). The hydrophobicity of the coating material was quantified using water contact angle measurement, in which the KZC1, KZC2 and KZC3 coatings show angles of  $\sim 121^\circ$ ,  $\sim 126^\circ$  and  $\sim 134^\circ$ , respectively, whereas the coating without ZNPs (KC) shows a contact angle of  $\sim 72^\circ$  (Fig. 5b) and the water contact angle of the ZNP was found to be  $\sim 80^\circ$  (Fig. S9). The coating composite of feather microfiber with ZNPs is proven to be hydrophobic as per the standards, whereas the coating of the feather microfiber alone could not match the same.<sup>71</sup> This improvement in the hydrophobicity can be attributed to the compaction of the layer with the nanoparticles as the nanofillers of the pores, and with the tight binding of the functional groups on the feather. In contrast, KC is hydrophilic with a porous morphology that cannot withstand water due to the presence of pores, which provide a pathway for water penetration. Thus, the compact nature of the material results in flexibility, hydrophobic properties, and uniformity in coating, with an increase in these values proportional to the amount of coating material used.

### Stability of the coated urea

To guarantee that the coating is suitable for industrial purposes such as storage and transportation, its stability must be ensured against penetration, abrasion, and humidity. The penetration study was carried out by placing the coated urea under a 70 g plunger. None of the coatings had any discernible penetration depth ( $\sim 0.4$ – $0.3$  mm penetration observed in KZC3, KZC2, and KZC1). This may be due to nanoscale dense fillers, which improve the hardness. On the other hand, bare urea pellets, further denoted as WC and KC, due to the absence of coating and nano-fillers, respectively, show penetration of up to  $\sim 0.6$  mm (Fig. 6a). Consequently, the material in KZC resists the penetrating force due to its relative compact-



**Fig. 5** (a) Young's modulus and (b) water contact angle with respective angle photographs of feather microfiber coated with urea as a control coating (KC) and three different feather microfiber zinc-coated urea samples with 3%, 6%, and 9% coating content (KZC1, KZC2, and KZC3), respectively.

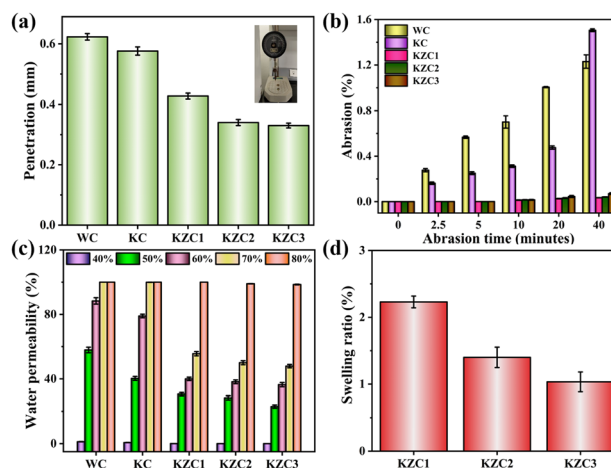


**Fig. 6** (a) Penetration distance (inset showing the penetrometer), (b) abrasion (%), and (c) water permeability (%) at different RH, and (d) swelling ratio (%) of uncoated urea (WC), feather microfiber coated urea (KC), and three different feather microfiber zinc-coated urea with 3%, 6%, and 9% coating content (KZC1, KZC2, and KZC3), respectively.

ness and elasticity, as measured by its Young's modulus. The abrasion resistance was measured by rotating coated and uncoated urea in a drum with zirconium beads, followed by gravimetric analysis at regular intervals after being sieved. The abrasion percentages increased over time in KZC, KC, and WC samples (Fig. 6b); at 40 minutes of abrasion time, the abrasion percentage of KC appears higher than that of bare urea pellets (WC). The KC initially provides a layer of coating, but it lacks structural stability and proper adhesion without the reinforcing effect of the ZNPs. Hence, the KC layer, although initially present, is prone to delamination and disintegration under abrasive stress, followed by urea fragmentation. The fragmented and less adherent KC material, once abraded, may contribute more to the measured "loss" than the control bare urea (WC), where the loss is found to be only through urea fragmentation. However, it was observed that KZC had negligible abrasion in relative terms. Furthermore, an increase in the coating material concentration did not have much effect on the abrasion for KZC, which may be due to the involvement of nano-fillers, because the control KC was susceptible to abrasion.

To check the stability of the coated urea in water, permeability tests were carried out at different relative humidity (RH). The coated and uncoated urea samples were kept at different RH for 20 days, and a gravimetric analysis was performed before and after exposure. At 40% RH, none of the urea demonstrated any visible dissolution. With a further increase in the humidity to 5%, the WC showed complete dissolution, but KC resisted the effect and resulted in 80% water accumulation. In contrast, from 50%–70% RH, the water permeability of KZC was  $\sim 38$ – $50$ % (Fig. 6c). Notably, it was observed that, at 80% RH incubation, the KZC-coated urea samples retained the compact morphology visually (Fig. S10), but were soft. This appears to be contradictory to the hydro-

phobicity trend because, even with the enhanced hydrophobicity and compactness due to ZNPs, the feather microfiber coating is still a biopolymer coating. Where the ZNPs reduce initial water penetration and fill the pores,<sup>72</sup> the remaining pores, even if initially small, can eventually become saturated at very high humidity (80% RH) over time. This water absorption, even if it does not lead to complete dissolution, causes the biopolymer matrix to swell. This swelling (Fig. 6d), in turn, can lead to a decrease in the polymer's rigidity, resulting in a "softening" effect.

The biodegradability of the feather microfiber is always a major concern; hence, a soil burial test was conducted in which the coating material was coated over a glass slide and then kept under soil. The coating content was examined over 60 days, resulting in ~70% degradation (Fig. 7a). This could be attributed to the pretreatment, involving dispersing the feathers in dilute acid followed by microwave heating, which alters their secondary structure with nano-fillers.

### Release profile of the coated urea

Following the confirmation of the suitability of the coating material for transport and storage, the release pattern was evaluated in water. To check the release, coated urea was incubated in distilled water, then water samples were collected at regular intervals to check the nitrogen release in the water by the Kjeldahl method. The results confirmed the complete dissolution of WC without any hindrance. Similarly, KC, due to sufficient water permeability, was not able to withstand for long and dissolved in the water. In contrast, KZC exhibited slow-release of the fertilizer, which may be due to the addition of nanoscale dense fillers that increase compactness. In KZC with different coating thicknesses, *viz.*, KZC3, KZC2, and KZC1, ~66%, 70%, and 84% release was observed after

5 hours, respectively (Fig. 7b). This outcome indicates that higher coating content may limit water penetration into the fertilizer, which causes slow nutrient release from the pellets of KZC2 and KZC3. Furthermore, to study the kinetics of the release, four mathematical models were used (Table 2), and the standard error of estimate (SER), diffusional exponent ( $R^2$ ), and diffusional exponent ( $n$ ) were calculated. The results revealed that the Ritger–Peppas model best fits the release mechanism with the highest  $R^2$  and lowest SER. The diffusional constant was found to be less than 0.5, proving that release follows a Fickian diffusion-controlled release that depends on the swelling and dissolution of the polymer matrix<sup>73,74</sup> (Fig. S11 and Table S2). Additionally, this could be linked to the softening and swelling of the coating material over time, which facilitates the diffusion of urea through the swollen polymer network. This facilitates protein degradation due to pH elevation, caused by urea within the coating, acting as a denaturing agent, leading to nitrogen and zinc release from the structure. From the above studies, it is found that KZC2 has a balance in the release, penetration resistance, and biodegradability; hence, for further volatilization and crop production evaluation, only this sample was taken forward and denoted as KZC. Two major losses are reported for urea, listed as leaching loss and volatilization loss. The release of nutrients in the soil was tested using a leaching test, where the same trend as the release study was observed with an extended duration. Thus, it was found that the leaching caused <15% loss in KZC, which is significantly less compared with those of WC and KC (~34% loss in KC, and ~53% loss in WC) (Fig. 7c). This extension in the duration is obviously due to the supplementary compaction given by the soil over the pellet and its coatings; KC also exhibited limited loss, although it is not as significant as the KZC samples. A volatilization loss study was conducted by incubating the coated and uncoated urea in a closed container for 24 hours at room temperature, and the loss of ammonia was estimated at 150 °C and 50% relative humidity using an ammonia gas sensor. This revealed that the KZC sample had ~74% and ~67% less ammonia volatilization compared to WC and KC, respectively (Fig. 7d).

### Pot study

A pot experiment with rice crops (Fig. S12) was conducted to check the effect of coated over uncoated urea on the growth of the plants. Rice cultivation particularly requires standing water during early growth stages. Therefore, a hydrophobic coating is essential to prevent premature urea dissolution. From all the above observations KZC2 stood up the best one for real time experiment by eliminating the other formulations further, denoted as KZC compared to WC. Pellets were applied as per the treatments listed in Table 3. After application, the crop was monitored until maturation, and the yield was calculated. It was found that the coated urea increased grain yield over the uncoated pellets by ~10% and ~15% in 2 and 3 splits of 100% recommended dose of nitrogen (RDN), respectively. Similar results *viz.*, an increase in the yield of ~5% and ~8% was observed in 2 and 3 splits, respectively, with 75% RDN



**Fig. 7** (a) Biodegradation in terms of weight loss, (b) cumulative release, (c) leaching loss, and (d) volatilization loss of uncoated urea (WC), feather microfiber coated urea (KC), and three different feather microfiber zinc-coated urea with 3%, 6%, and 9% coating content (KZC1, KZC2, and KZC3), respectively.



**Fig. 8** (a) Increased yield (%) over control (uncoated urea), (b) N%, (c) SPAD value, and (d) ZUE ( $\text{g mg}^{-1}$ ) in different treatments.

(Fig. 8a). However, it was observed that 2 splits of 100% and 75% RDN had less impact on the yield. A possible reason could be that reducing the number of applications of fertilizer leads to heat shock in the root zone<sup>16</sup> as reported for the application of urea, causing a relative decrease in yield. A comprehensive assessment of crop growth was conducted by determining the total dry weight of the above-ground parts (leaves, stems, and grains), known as biological yield. The biological yield and harvest index were found to be correlated to the grain yield, as depicted in Fig. S13a and S13b, respectively. The N content was calculated in the (above-ground) vegetative parts by the Kjeldahl method to understand the underlying reasons. It was noticed that within both recommended doses, after 60 days, the N content increased with increasing number of splits, leading to a steady nitrogen availability, while in the initial 30 days at a lower recommended dose (75%), there was no such effect of reducing the number of splits (Fig. 8b). This pattern shows similarity with the yield result, *i.e.*, nearly similar increase in the yield with 75% RDN. A non-destructive chlorophyll content measurement using a SPAD meter vali-

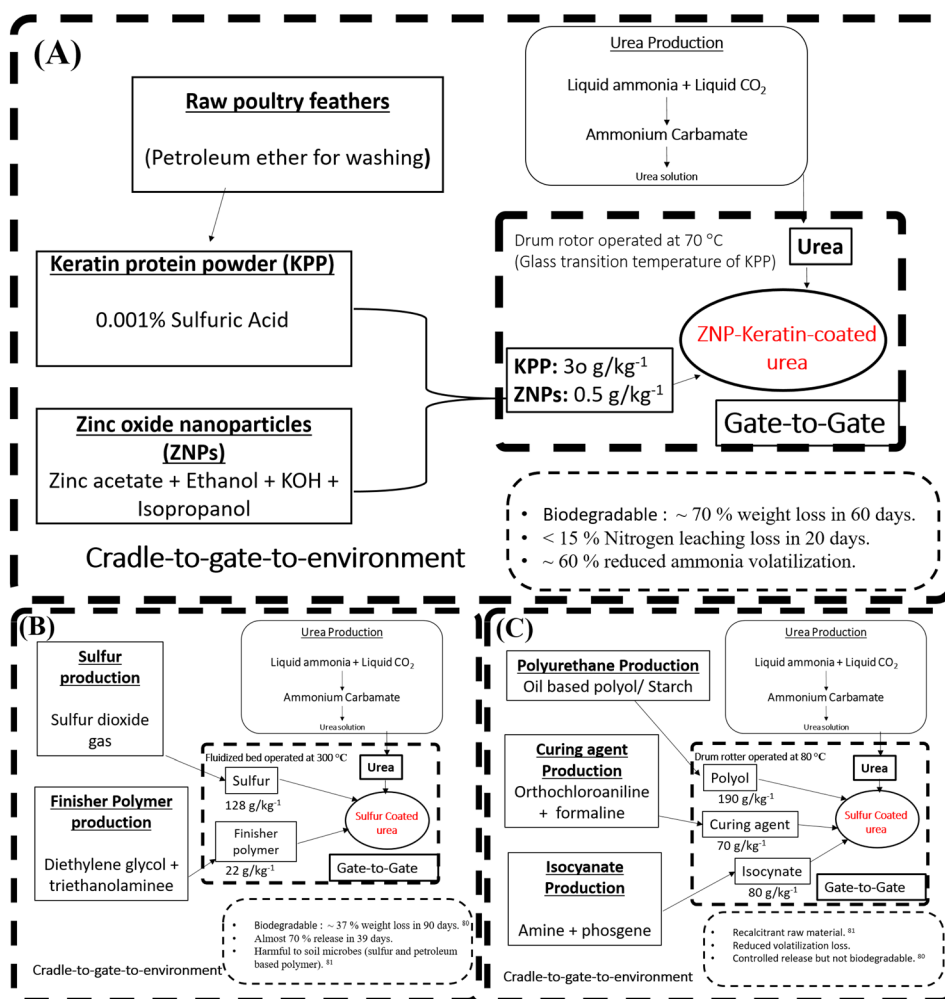


**Fig. 9** Boundary of (A) 6% feather microfiber zinc-coated urea (KZC), (B) sulfur-coated urea, and (C) polymer-coated urea in cradle-to-gate-to-environment life cycle analysis.

dated the N content on the 30<sup>th</sup> and 60<sup>th</sup> days after transplanting. It was observed that, after 60 days, there was an increase in chlorophyll content with 3 splits, validating the N increase and yield (Fig. 8c). Zinc, as a micronutrient for plants, plays a critical role as a cofactor in physiological functions and also affects the yield of the crops.<sup>37</sup> As zinc forms part of the coating framework, its content was determined by the wet-digestion method. Zinc utilization efficiency (ZUE) results showed better uptake of zinc with an increased number of splits, confirming the simultaneous uptake of both N and Zn, which can be another reason for the increase in yield. This indicates that the level of ZNPs used in our coating material is considered beneficial for plant growth and is not expected to cause toxicity (Fig. 8d).

### Life cycle assessment (LCA)

The LCA results revealed that KZC exhibits significantly less environmental burden across all major impact categories compared to both well-known sulfur- and polymer-coated urea<sup>75,76</sup> (Fig. 9 and Table S3). For global and marine ecotoxicity, the KZC reduced emissions by up to 11 times, primarily due to its minimal use of synthetic polymers and reliance on valorized poultry feather waste. Ozone formation impacts were lowered by 4–7 times, indicating improved air quality potential. Human carcinogenic toxicity and freshwater ecotoxicity were also remarkably lowered up to 11.9 and 9.7 times, respectively. The greatest contrast was observed in terrestrial acidification, where the KZC showed reductions of over 7700–13 800 times, highlighting the benefit of eliminating high-sulfur coatings. Although terrestrial ecotoxicity remained relatively high (41 kg 1,4-DCB eq), it was still found to be lower than that of sulfur and polymer-coated urea by factors of 2.2 and 2.9, respectively, suggesting improved but still impactful residue handling. Finally, based on the life cycle impact assessment (LCIA) data, it has been proven that the developed coating significantly lowers the overall environmental impact, offering a promising route to sustainable urea fertilizer solutions.

## Conclusions

Earlier, fossil-fuel-based polymers were commonly used for fertilizer coating due to their low cost and film-forming ability to prevent dissolution. This study demonstrates a sustainable biopolymer alternative, where, a fertilizer coating based on waste feather microfibers is pursued without using any binder. By employing mild heat, which causes a dense glassy state that facilitates binding to the nanoparticles and eliminates the need for expensive synthetic polymer binders. Thus, the assembled feather-based microfiber coating was able to meet industry requirements such as abrasion and humidity resistance. Finally, the fertilizer also delivered a slow release of the nutrient to the soil and increased the rice yield. Biodegradation studies show the absence of remnants in the soil for longer periods of time. However, in future field studies, diverse irrigation regimes are necessary to comprehen-

sively evaluate the long-term persistence and performance of the coating. The use of waste protein after acid hydrolysis followed by microwave-assisted thermal treatment represents a significant step towards scalability, since domestic microwaves can be replaced with industrial microwave systems. The rapid and volumetric heating capability of microwaves can significantly reduce processing time compared to lab-limited procedures. However, variations in the feather source or large-scale ZnO synthesis and dispersion could influence coating consistency. Quality control measures during scale-up would be crucial to mitigate such variation. The use of waste feather biopolymers and the binder-free approach inherently suggest the cost-effective and environmentally friendly nature of the process, since the given treatments shorten the active processing time compared to traditional methods that can require toxic chemicals such as 2-mercaptoethanol and L-cysteine. This contributes an industrial-friendly step of the proposed coating by reducing the hazardous wastes, associated disposal costs and lowering the environmental burden compared with the marketed polymer and sulphur-coated fertilizers, offering a promising way towards sustainable urea fertilizer solutions.

## Author contributions

Kanchan Swami: performed the experiments, analysed the data, writing – review & editing; Mona Nagargade and Vishal Tyagi: conducted pot experiment and performed nutrients analysis; Parul Sharma and Prem Kumar: review & editing, assisted in experiments; Bandana Kumari Sahu, Navjot Singh: assisted in pot experiment; Sarita Kataria: performed Raman spectroscopy; Vijayakumar Shanmugam: conceptualisation, resources, supervision, and writing – review & editing.

## Conflicts of interest

There are no conflicts to declare.

## Data availability

The data supporting this article have been included as part of the supplementary information (SI). Supplementary information is available. See DOI: <https://doi.org/10.1039/d5gc04420k>.

## Acknowledgements

V. S. acknowledges DBT BT/PR36476/NNT/28/1723/2020, Government of India. K. S. is grateful to the DBT for the fellowship and the INST for the instrument facility.

## References

- 1 R. Lee, The outlook for population growth, *Science*, 2011, **333**(6042), 569–573.
- 2 D. A. Daramola and M. C. Hatzell, Energy demand of nitrogen and phosphorus based fertilizers and approaches to circularity, *ACS Energy Lett.*, 2023, **8**(3), 1493–1501.
- 3 T. T. Pham, X. Chen, T. Söhnle, N. Yan and J. Sperry, Haber-independent, diversity-oriented synthesis of nitrogen compounds from biorenewable chitin, *Green Chem.*, 2020, **22**(6), 1978–1984.
- 4 D. Coskun, D. T. Britto, W. Shi and H. J. Kronzucker, Nitrogen transformations in modern agriculture and the role of biological nitrification inhibition, *Nat. Plants*, 2017, **3**(6), 1–0.
- 5 D. Wang, B. Li, J. Ma, J. Wang, H. Wang and W. Li, Pseudoplastic liquid mulch film incorporating waste lignin and starch to improve its sprayability and available soil nitrogen, *Chem. Eng. J.*, 2023, **475**, 146392.
- 6 H. M. Ye, H. F. Li, C. S. Wang, J. Yang, G. Huang, X. Meng and Q. Zhou, Degradable polyester/urea inclusion complex applied as a facile and environment-friendly strategy for slow-release fertilizer: Performance and mechanism, *Chem. Eng. J.*, 2020, **381**, 122704.
- 7 D. Qiao, H. Liu, L. Yu, X. Bao, G. P. Simon, E. Petinakis and L. Chen, Preparation and characterization of slow-release fertilizer encapsulated by starch-based superabsorbent polymer, *Carbohydr. Polym.*, 2016, **147**, 146–154.
- 8 Y. C. Yang, M. Zhang, Y. Li, X. H. Fan and Y. Q. Geng, Improving the quality of polymer-coated urea with recycled plastic, proper additives, and large tablets, *J. Agric. Food Chem.*, 2012, **60**(45), 11229–11237.
- 9 H. Tian, Z. Liu, M. Zhang, Y. Guo, L. Zheng and Y. C. Li, Biobased polyurethane, epoxy resin, and polyolefin wax composite coating for controlled-release fertilizer, *ACS Appl. Mater. Interfaces*, 2019, **11**(5), 5380–5392.
- 10 M. Tomaszewska and A. Jarosiewicz, Use of polysulfone in controlled-release NPK fertilizer formulations, *J. Agric. Food Chem.*, 2002, **50**(16), 4634–4639.
- 11 X. Zhao, X. Qi, Q. Chen, X. Ao and Y. Guo, Sulfur-modified coated slow-release fertilizer based on castor oil: synthesis and a controlled-release model, *ACS Sustainable Chem. Eng.*, 2020, **8**(49), 18044–18053.
- 12 H. Tian, Z. Li, P. Lu, Y. Wang, C. Jia, H. Wang, Z. Liu and M. Zhang, Starch and castor oil mutually modified, cross-linked polyurethane for improving the controlled release of urea, *Carbohydr. Polym.*, 2021, **251**, 117060.
- 13 L. Xie, M. Liu, B. Ni and Y. Wang, Utilization of wheat straw for the preparation of coated controlled-release fertilizer with the function of water retention, *J. Agric. Food Chem.*, 2012, **60**(28), 6921–6928.
- 14 X. Ma, J. Chen, Y. Yang, X. Su, S. Zhang, B. Gao and Y. C. Li, Siloxane and polyether dual modification improves hydrophobicity and interpenetrating polymer network of bio-polymer for coated fertilizers with enhanced slow release characteristics, *Chem. Eng. J.*, 2018, **350**, 1125–1134.
- 15 S. Zhang, X. Fu, Z. Tong, G. Liu, S. Meng, Y. Yang, M. I. Helal and Y. C. Li, Lignin–clay nanohybrid biocomposite-based double-layer coating materials for controllable-release fertilizer, *ACS Sustainable Chem. Eng.*, 2020, **8**(51), 18957–18965.
- 16 B. K. Sahu, M. Nagargade, M. Chandel, K. Kaur, K. Swami, P. Kumar, M. Palanisami, A. D. Pathak, S. K. Shukla and V. Shanmugam, Eco-friendly urea nanosack: jute grafted silica nanoring woven fertilizer to control urea release and enhance crop productivity, *ACS Sustainable Chem. Eng.*, 2022, **10**(40), 13357–13366.
- 17 M. J. Gan, Y. Q. Niu, X. J. Qu and C. H. Zhou, Lignin to value-added chemicals and advanced materials: extraction, degradation, and functionalization, *Green Chem.*, 2022, **24**(20), 7705–7750.
- 18 K. Swami, B. K. Sahu, M. Nagargade, K. Kaur, A. D. Pathak, S. K. Shukla, T. Stobdan and V. Shanmugam, Starch wall of urea: Facile starch modification to residue-free stable urea coating for sustained release and crop productivity, *Carbohydr. Polym.*, 2023, **317**, 121042.
- 19 T. N. Le, K. Robertson, M. Escribà-Gelonch, P. Marschner, N. N. Tran, P. M. Williams, I. Fisk and V. Hessel, Microflow synthesis of a formulation of phosphorus fertiliser to enhance the P content in soil and P uptake in wheat, *Green Chem.*, 2023, **25**(22), 9422–9437.
- 20 T. N. Le, C. N. Lim, I. Fisk, N. N. Tran, V. Hessel and K. Robertson, Sustainable fertiliser mesh, '4D'-precision engineered by flow chemistry: minimising agrochemical pollution, *Green Chem.*, 2025, **27**(3), 696–715.
- 21 F. Allievi, M. Vinnari and J. Luukkanen, Meat consumption and production—analysis of efficiency, sufficiency and consistency of global trends, *J. Cleaner Prod.*, 2015, **92**, 142–151.
- 22 L. Gao, H. Hu, X. Sui, C. Chen and Q. Chen, One for two: Conversion of waste chicken feathers to carbon microspheres and (NH<sub>4</sub>) HCO<sub>3</sub>, *Environ. Sci. Technol.*, 2014, **48**(11), 6500–6507.
- 23 N. Reddy, L. Chen, Y. Zhang and Y. Yang, Reducing environmental pollution of the textile industry using keratin as alternative sizing agent to poly (vinyl alcohol), *J. Cleaner Prod.*, 2014, **65**, 561–567.
- 24 A. J. Poole, J. S. Church and M. G. Huson, Environmentally sustainable fibers from regenerated protein, *Biomacromolecules*, 2009, **10**(1), 1–8.
- 25 K. M. Arai, R. Takahashi, Y. Yokote and K. Akahane, Amino-acid sequence of feather keratin from fowl, *Eur. J. Biochem.*, 1983, **132**(3), 501–507.
- 26 B. Ma, X. Qiao, X. Hou and Y. Yang, Pure keratin membrane and fibers from chicken feather, *Int. J. Biol. Macromol.*, 2016, **89**, 614–621.
- 27 B. Mu, F. Hassan and Y. Yang, Controlled assembly of secondary keratin structures for continuous and scalable production of tough fibers from chicken feathers, *Green Chem.*, 2020, **22**(5), 1726–1734.
- 28 M. Harris and A. E. Brown, Natural and synthetic protein fibers, *Text. Res. J.*, 1947, **17**(6), 323–330.

- 29 H. Xu and Y. Yang, Controlled de-cross-linking and disentanglement of feather keratin for fiber preparation via a novel process, *ACS Sustainable Chem. Eng.*, 2014, **2**(6), 1404–1410.
- 30 B. Zhou and H. L. Wang, The optimization of regeneration feather protein/PVA composite fiber's production technology using gray clustering analysis, *Adv. Mater. Res.*, 2011, **332**, 500–504.
- 31 P. M. Schrooyen, P. J. Dijkstra, R. C. Oberthür, A. Bantjes and J. Feijen, Partially carboxymethylated feather keratins. 1. Properties in aqueous systems, *J. Agric. Food Chem.*, 2000, **48**(9), 4326–4334.
- 32 J. R. Barone, W. F. Schmidt and N. T. Gregoire, Extrusion of feather keratin, *J. Appl. Polym. Sci.*, 2006, **100**(2), 1432–1442.
- 33 Y. Yu, W. Yang and M. A. Meyers, Viscoelastic properties of  $\alpha$ -keratin fibers in hair, *Acta Biomater.*, 2017, **64**, 15–28.
- 34 B. S. Sooraj, J. Roy, M. Mukherjee, A. Jose and T. Pradeep, Extensive Polymerization of Atomically Precise Alloy Metal Clusters During Solid-State Reactions, *Langmuir*, 2024, **40**(29), 15244–15251.
- 35 L. M. Gilbertson and P. J. Vikesland, Inspiring a nanocircular economy, *Environ. Sci.: Nano*, 2022, **9**(3), 839–840.
- 36 A. Moezzi, A. M. McDonagh and M. B. Cortie, Zinc oxide particles: Synthesis, properties and applications, *Chem. Eng. J.*, 2012, **185**, 1–22.
- 37 J. A. Hernandez-Viezcas, H. Castillo-Michel, A. D. Servin, J. R. Peralta-Video and J. L. Gardea-Torresdey, Spectroscopic verification of zinc absorption and distribution in the desert plant *Prosopis juliflora-velutina* (velvet mesquite) treated with ZnO nanoparticles, *Chem. Eng. J.*, 2011, **170**(2–3), 346–352.
- 38 Y. Li, J. Zhao, Q. Hu, T. Hao, H. Cao, X. Huang, Y. Liu, Y. Zhang, D. Lin, Y. Tang and Y. Cai, Prussian blue analogs cathodes for aqueous zinc ion batteries, *Mater. Today Energy*, 2022, **29**, 101095.
- 39 W. Maret and Y. Li, Coordination dynamics of zinc in proteins, *Chem. Rev.*, 2009, **109**(10), 4682–4707.
- 40 T. W. Chang, H. Ko, W. S. Huang, Y. C. Chiu, L. X. Yang, Z. C. Chia, Y. C. Chin, Y. J. Chen, Y. T. Tsai, C. W. Hsu, C. C. Chang, P. J. Tsai and C. C. Huang, Tannic acid-induced interfacial ligand-to-metal charge transfer and the phase transformation of Fe<sub>3</sub>O<sub>4</sub> nanoparticles for the photothermal bacteria destruction, *Chem. Eng. J.*, 2022, **428**, 131237.
- 41 C. Stanton, D. Sanders, U. Krämer and D. Podar, Zinc in plants: Integrating homeostasis and biofortification, *Mol. Plant*, 2022, **15**(1), 65–85.
- 42 C. Andreini, I. Bertini and A. Rosato, Metalloproteomes: a bioinformatic approach, *Acc. Chem. Res.*, 2009, **42**(10), 1471–1479.
- 43 P. Sharma, B. K. Sahu, K. Swami, M. Chandel, P. Kumar, T. Palanisamy and V. Shanmugam, E-seed skin: a carbohydrate–protein hybrid nanostructure for delayed germination and accelerated growth, *J. Mater. Chem. B*, 2025, **13**(12), 3895–3905.
- 44 C. Cabot, S. Martos, M. Llugany, B. Gallego, R. Tolrà and C. Poschenrieder, A role for zinc in plant defense against pathogens and herbivores, *Front. Plant Sci.*, 2019, **10**, 1171.
- 45 M. S. Lee, G. P. Gippert, K. V. Soman, D. A. Case and P. E. Wright, Three-dimensional solution structure of a single zinc finger DNA-binding domain, *Science*, 1989, **245**(4918), 635–637.
- 46 M. Yang, S. Li, S. Zhang, B. Gao, Z. Tong, D. Cheng, D. Chen, R. Huang and Y. Yang, Dense and superhydrophobic biopolymer-coated large tablet produced with energy efficient UV-curing for controlled-release fertilizer, *J. Mater. Chem. A*, 2022, **10**(36), 18834–18844.
- 47 S. Zhang, Y. Yang, B. Gao, Y. C. Li and Z. Liu, Superhydrophobic controlled-release fertilizers coated with bio-based polymers with organosilicon and nano-silica modifications, *J. Mater. Chem. A*, 2017, **5**(37), 19943–19953.
- 48 X. C. Yin, F. Y. Li, Y. F. He, Y. Wang and R. M. Wang, Study on effective extraction of chicken feather keratins and their films for controlling drug release, *Biomater. Sci.*, 2013, **1**(5), 528–536.
- 49 ASTM. Annual Book of ASTM Standards, 1990: Subject Index; Alphanumeric List. American Society for Testing & Materials.
- 50 G. R. Moore, S. M. Martelli, C. Gandolfo, P. J. do Amaral Sobral and J. B. Laurindo, Influence of the glycerol concentration on some physical properties of feather keratin films, *Food Hydrocolloids*, 2006, **20**(7), 975–982.
- 51 M. Gaceur, S. B. Dkhil, D. Duché, F. Bencheikh, J. J. Simon, L. Escoubas, M. Mansour, A. Guerrero, G. Garcia-Belmonte, X. Liu and M. Fahlman, Ligand-Free Synthesis of Aluminum-Doped Zinc Oxide Nanocrystals and their Use as Optical Spacers in Color-Tuned Highly Efficient Organic Solar Cells, *Adv. Funct. Mater.*, 2016, **26**(2), 243–253.
- 52 United Nations Industrial Development Organization, International Fertilizer Development Center. *Fertilizer manual*, Kluwer, 1998.
- 53 Y. Zhang, X. Liang, X. Yang, H. Liu and J. Yao, An eco-friendly slow-release urea fertilizer based on waste mulberry branches for potential agriculture and horticulture applications, *ACS Sustainable Chem. Eng.*, 2014, **2**(7), 1871–1878.
- 54 C. G. Chiaregato and R. Faez, Micronutrients encapsulation by starch as an enhanced efficiency fertilizer, *Carbohydr. Polym.*, 2021, **271**, 118419.
- 55 L. Liu, Y. Ni, Y. Zhi, W. Zhao, M. Pudukudy, Q. Jia, S. Shan, K. Zhang and X. Li, Sustainable and biodegradable copolymers from SO<sub>2</sub> and renewable eugenol: a novel urea fertilizer coating material with superior slow release performance, *Macromolecules*, 2020, **53**(3), 936–945.
- 56 E. C. Humphries, *Moderne Methoden der Pflanzenanalyse/Modern Methods of Plant Analysis: Erster Band/Volume I, in Mineral components and ash analysis*, 1956, pp. 468–502.
- 57 J.-B. Zhou, J.-G. Xi, Z.-J. Chen and S.-X. Li, *Leaching and transformation of nitrogen fertilizers in soil after application of N with irrigation: a soil column method*, 2006.

- 58 P. Kumar, M. Chandel, S. Kataria, K. Swami, K. Kaur, B. K. Sahu, A. Dadhich, R. R. Urkude, K. Subaharan, N. Koratkar and V. Shanmugam, Handheld crop pest sensor using binary catalyst-loaded nano-SnO<sub>2</sub> particles for oxidative signal amplification, *ACS Sens.*, 2023, **9**(1), 81–91.
- 59 Y. S. Shivay, R. Prasad and M. Pal, Effects of source and method of zinc application on yield, zinc biofortification of grain, and Zn uptake and use efficiency in chickpea (*Cicer arietinum* L.), *Commun. Soil Sci. Plant Anal.*, 2015, **46**(17), 2191–2200.
- 60 B. K. Sahu, K. Swami, N. Kapoor, A. Agrawal, S. Kataria, P. Sharma, P. Kundu, H. Thangavel, A. Vattakkuniyil, O. P. Chaurasia and V. Shanmugam, Soil-mimetic eco-friendly fertilizer gates: nanoclay-reinforced binary carbohydrates for improving crop efficiency, *Environ. Sci.: Nano*, 2024, **11**(7), 3006–3018.
- 61 A. Ullah, T. Vasanthan, D. Bressler, A. L. Elias and J. Wu, Bioplastics from feather quill, *Biomacromolecules*, 2011, **12**(10), 3826–3832.
- 62 C. D. Tran, F. Proscenc, M. Franko and G. Benzi, Synthesis, structure and antimicrobial property of green composites from cellulose, wool, hair and chicken feather, *Carbohydr. Polym.*, 2016, **151**, 1269–1276.
- 63 P. Sun, Z. T. Liu and Z. W. Liu, Particles from bird feather: A novel application of an ionic liquid and waste resource, *J. Hazard. Mater.*, 2009, **170**(2–3), 786–790.
- 64 G. Yang, Q. Chen, D. Wen, Z. Chen, J. Wang, G. Chen, Z. Wang, X. Zhang, Y. Zhang, Q. Hu and L. Zhang, A therapeutic microneedle patch made from hair-derived keratin for promoting hair regrowth, *ACS Nano*, 2019, **13**(4), 4354–4360.
- 65 K. Elumalai and S. Velmurugan, Green synthesis, characterization and antimicrobial activities of zinc oxide nanoparticles from the leaf extract of *Azadirachta indica* (L.), *Appl. Surf. Sci.*, 2015, **345**, 329–336.
- 66 T. Varadavenkatesan, E. Lyubchik, S. Pai, A. Pugazhendhi, R. Vinayagam and R. Selvaraj, Photocatalytic degradation of Rhodamine B by zinc oxide nanoparticles synthesized using the leaf extract of *Cyanometra ramiflora*, *J. Photochem. Photobiol., B*, 2019, **199**, 111621.
- 67 C. D. Tran and T. M. Mututuvari, Cellulose, chitosan and keratin composite materials: Facile and recyclable synthesis, conformation and properties, *ACS Sustainable Chem. Eng.*, 2016, **4**(3), 1850–1861.
- 68 J. T. Pelton and L. R. McLean, Spectroscopic methods for analysis of protein secondary structure, *Anal. Biochem.*, 2000, **277**(2), 167–176.
- 69 B. Yuan, H. Li, H. Hong, Q. Wang, Y. Tian, H. Lu, J. Liu, L. Lin, G. Wu and C. Yan, Immobilization of lead(II) and zinc(II) onto glomalin-related soil protein (GRSP): Adsorption properties and interaction mechanisms, *Ecotoxicol. Environ. Saf.*, 2022, **236**, 113489.
- 70 C. Zhao, J. Niu, C. Xiao, Z. Qin, X. Jin, W. Wang and Z. Zhu, Separator with high ionic conductivity and good stability prepared from keratin fibers for supercapacitor applications, *Chem. Eng. J.*, 2022, **444**, 136537.
- 71 F. Wang, R. Chang, R. Ma, H. Qiu and Y. Tian, Eco-friendly and pH-responsive nano-starch-based superhydrophobic coatings for liquid-food residue reduction and freshness monitoring, *ACS Sustainable Chem. Eng.*, 2021, **9**(30), 10142–10153.
- 72 P. L. Ritger and N. A. Peppas, A simple equation for description of solute release II. Fickian and anomalous release from swellable devices, *J. Controlled Release*, 1987, **5**(1), 37–42.
- 73 V. S. Mesias, A. B. Agu, P. J. Benablo, C. H. Chen and D. P. Penaloza Jr, Coated NPK fertilizer based on citric acid-crosslinked chitosan/alginate encapsulant, *J. Ecol. Eng.*, 2019, **20**(11), 1–2.
- 74 C. G. Chiaregato, D. França, L. L. Messa, T. dos Santos Pereira and R. Faez, A review of advances over 20 years on polysaccharide-based polymers applied as enhanced efficiency fertilizers, *Carbohydr. Polym.*, 2022, **279**, 119014.
- 75 X. Liu, Y. Yang, B. Gao, Y. Li and Y. Wan, Environmentally friendly slow-release urea fertilizers based on waste frying oil for sustained nutrient release, *ACS Sustainable Chem. Eng.*, 2017, **5**(7), 6036–6045.
- 76 L. P. Lamers, L. L. Govers, I. C. Janssen, J. J. Geurts, M. E. Van der Welle, M. M. Van Katwijk, T. Van der Heide, J. G. Roelofs and A. J. Smolders, Sulfide as a soil phytotoxin—a review, *Front. Plant Sci.*, 2013, **4**, 268.